Sustainable Energy & Fuels

Sequential hydrogen production system from formic acid and H_2/CO_2 separation under high-pressure conditions

Journal:	*Sustainable Energy & Fuels*
Manuscript ID	SE-ART-02-2018-000087.R2
Article Type:	Paper
Date Submitted by the Author:	17-May-2018

Complete List of Authors:	Iguchi, Masayuki; National Institute of Advanced Industrial Science and Technology, Research Institute for Chemical Process Technology Chatterjee, Maya; National Institute of Advanced Industrial Science and Technology, Research Institute for Chemical Process Technology Onishi, Naoya; National Institute of Advanced Industrial Science and Technology, Department of Department of Energy and Environment Himeda, Yuichiro; National Institute of Advanced Industrial Science and Technology, Department of Energy and Environmental Kawanami, Hajime; National Institute of Advanced Industrial Science and Technology, Research Institute for Chemical Process Technology

Journal Name

ARTICLE

Sequential hydrogen production system from formic acid and H_2/CO_2 separation under high-pressure conditions

Received 00th January 20xx,
Accepted 00th January 20xx

DOI: 10.1039/x0xx00000x

www.rsc.org/

Masayuki Iguchi,[a] Maya Chatterjee,[a] Naoya Onishi,[b] Yuichiro Himeda[b] and Hajime Kawanami*[a]

Hydrogen (H_2) production from formic acid (FA) is highly attractive regarding as a sustainable energy carrier by the interconversion between CO_2 and FA. The dehydrogenation of FA at high pressures can give advantages over the reaction at atmospheric condition for the separation of H_2 and CO_2 after the reaction and the volumetric energy density of H_2. We demonstrated the continuous production of high-pressure H_2 by catalytic decomposition of FA, and subsequent separation of H_2 and CO_2 from FA decomposition gas (H_2:CO_2 = 1:1) using the phase change phenomenon at low temperatures while maintaining the pressure. The iridium aqua complex coordinated with a bidentate pyridyl-imidazoline ligand catalyzed the dehydrogenation of FA with high efficiency at the pressure as high as 153 MPa. The Ir catalyst was found to be stable under continuous addition of neat FA at high pressures. The generation time and rate of high-pressure H_2 were controlled by feeding neat FA to the aqueous reaction system. Using our combined system, more than 99 mol% of H_2 (96 mol% of purity) and 94 mol% of CO_2 (99mol% of purity) were separately obtained from FA as a gas and liquid, respectively, under the high-pressure conditions without any mechanical compression.

Introduction

Sustainable development of our society has been claimed to utilize the renewable energy and carbon dioxide (CO_2), since we faced the depletion of fossil fuels and the increasing levels of CO_2 in the atmosphere. Molecular hydrogen (H_2) is considered as a clean alternative energy, but its gaseous nature inhibits the direct storage and long distance delivery.[1-4] In these days, formic acid (FA, HCO_2H) has attracted much attentions as one of liquid organic hydrogen carriers (LOHCs) because of easy handling and transporting to a large extent by using the present infrastructures.[5-11] FA is a stable liquid at ambient conditions and has a moderately high H_2 content among LOHCs such as methylcyclohexane. The production of FA can be made either from biomass or directly by the catalytic conversion of CO_2 in solvents.[12-14] The FA/CO_2 system as a hydrogen carrier promises a carbon-neutral and environmentally benign method (Figure 1). The H_2 production from FA (dehydrogenation, Eq. 1) has the low reaction enthalpy compared to other potential hydrogen carrier materials,[15] and the dehydrogenation of FA is a thermodynamically favourable reaction, which can occur at mild temperatures, even under high-pressure conditions, but the side reaction of FA decomposition (dehydration, Eq. 2) is also thermodynamically favourable.[15] Hence, an effective catalyst is required for the selective production of H_2 from FA suppressing the side reaction. In addition, the effective separation of H_2 and CO_2 after the reaction is necessary, not only for the utilization of H_2 but also for CO_2, which could be the starting material to variety of compounds including FA through the hydrogenation (Figure 1).

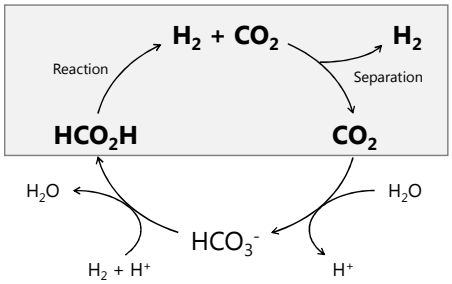

Figure 1. System of H_2 production from FA and storage with CO_2.

Mostly, H_2 has its application in the transportation sector to generate electricity by fuel cells. Some research groups have examined the application of H_2 produced from FA to a proton exchange membrane (PEM) fuel cell.[5, 16-21] The selective FA dehydrogenation is vital for the PEM fuel cell applications because the electro-catalyst involved in the cell can be easily deactivated by CO that is generated from the side reaction of FA decomposition (Eq. 2).[22, 23] The presence of CO_2 can also affect the PEM fuel cell performance at high current density due to the formation of CO via the reverse water-gas shift

[a] Research Institute for Chemical Process Technology, Department of Material and Chemistry, National Institute of Advanced Industrial Science and Technology, Nigatake 4-2-1, Miyagino-ku, Sendai, Miyagi 983-8551, Japan
[b] Research Institute of Energy Frontier, Department of Energy and Environment, National Institute of Advanced Industrial Science and Technology, Higashi 1-1-1, Tsukuba, Ibaraki 305-8565, Japan

Electronic Supplementary Information (ESI) available: See DOI: 10.1039/x0xx00000x

$$HCO_2H(l) \longrightarrow H_2(g) + CO_2(g) \quad \Delta G^\circ = -32.9 \text{ kJ/mol} \quad (1)$$

$$HCO_2H(l) \longrightarrow H_2O(l) + CO(g) \quad \Delta G^\circ = -12.4 \text{ kJ/mol} \quad (2)$$

reaction.[21-24] Therefore, CO_2 removal from H_2 is necessary for storage and application in the PEM fuel cells.

The relevant separation methods of H_2 and CO_2 are adsorption, absorption, use of membranes and low-temperature distillation.[25] High-pressure conditions can enhance the efficiency of H_2/CO_2 separation, the volumetric energy density of H_2, and handling of CO_2 for its delivery and storage, and further reaction with H_2 to produce FA (hydrogenation of CO_2). Furthermore, the pressurization and subsequent dehydrogenation of FA in the liquid state avoids the large amount of energy required for generating high-pressure H_2 (as much as 10-15 % of its energy content)[26]. Thus, the sequential production of H_2 from FA and H_2/CO_2 separation at high pressures can offer the energy-efficient process rather than that at atmospheric pressure. The high-pressure process relies on the development of suitable catalyst to generate high-pressure H_2 at mild temperatures.

Since the selective decomposition of FA into H_2 and CO_2 was performed under mild temperatures,[27, 28] many homogeneous and heterogeneous catalysts have been developed.[5-10] Especially, iridium-based catalysts showed relatively higher activity and stability in water (Turnover number (TON) > 2×10^6).[29, 30] However, there are few literatures for the high-pressure H_2 production from FA at less than 100 °C.[18, 27, 31-35] We recently demonstrated the high-pressure gas generation up to 123 MPa by the dehydrogenation of FA using the Cp^*Ir^{III} complexes (Cp^* = pentamethylcyclopentadienyl, **1** and **2** in Figure 2) at 80 °C.[36, 37] The reaction rate was largely decreased with an increase in the generated gas pressure by FA decomposition especially above 10 MPa.[38] Some highly active catalysts for the dehydrogenation of FA at atmospheric pressure quickly lost its activity at high pressures.[39] During the reaction at high pressures, the catalyst needs to be stable, especially under concentrated H_2, CO_2 and formic acid. Hence, the highly active and durable catalyst is required for the efficient production of high-pressure H_2 from FA.

In practical applications, H_2 should be produced by the catalytic decomposition of FA on demand. Either the reaction temperature or the FA concentration in reaction solution can control the H_2 production considering its storage and handling. The decomposition of FA accelerates at higher temperature, however, the increasing temperature causes the catalyst deactivation and complicated apparatus for evaporation of solvents during the reaction.[17, 40] The rate of FA dehydrogenation linearly related to the substrate concentration,[38] and the addition of substrate can be conducted using a liquid pump. Thus, the reaction time and rate of H_2 generation is easier to control by modulating the FA concentration rather than temperature. The addition of neat FA to the catalyst solution allows to full use of hydrogen density of FA. Several studies were reported for the H_2 production by continuous decomposition of FA at atmospheric pressure,[17-19, 40-43] but only a few studies focused on the continuous production of H_2 from FA at high pressures.[31]

In our previous work, the Cp^*Ir^{III} complex having 2-(2'-pyridyl)imidazoline as *N*,*N*'-bidentate ligand (**3** in Figure 2) was found to show the high activity and stability for the catalytic dehydrogenation of FA under atmospheric conditions.[44] Herein, we investigated the control of high-pressure H_2 generation time and rate by feeding neat FA to the aqueous reaction system using the catalyst **3** at mild temperatures. Furthermore, the efficient separation of H_2 and CO_2 after the reaction was studied using the phase change phenomenon of FA decomposition gas (H_2:CO_2 = 1:1) under high-pressure and low-temperature conditions.

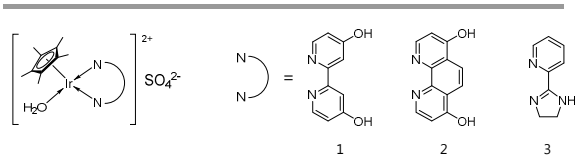

Figure 2. Ir aqua complex catalysts for FA dehydrogenation at high pressures.

Results and Discussion

The high-pressure gas generation from FA was studied using the catalyst **3** in a batch-wise operation (Figure 3). When 20 mol/L FA aqueous solution was used, the gas pressure reached to 153 MPa in 5 h at 80 °C. The final conversion of FA was calculated as 90 mol% at 153 MPa, and the high-pressure gas was composed of equimolar H_2 and CO_2 with quite low concentration of CO (<6 vol. ppm). Under the same condition, the attained pressure using **1** was lower (123 MPa)[36] than that of **3**, which indicates that **3** is more stable and active catalyst than **1** under the high-pressure conditions with H_2 and CO_2. In our previous work, we suggested that the catalyst deactivation of **1** is related to change in the chelating conformation by the rotation around pyridyl-pyridyl bond of bipyridine ligand in the complex.[37, 39]

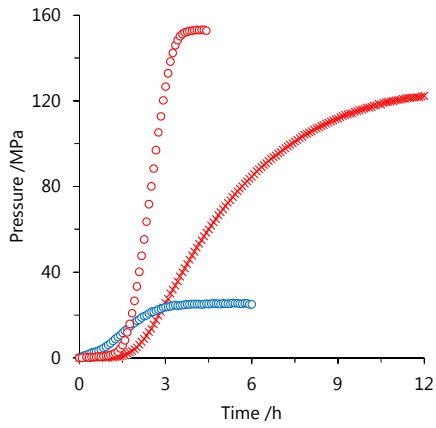

Figure 3. Time course of high-pressure gas generation by FA decomposition using the catalyst: **1** (cross), **3** (circle); 80 °C and 20 mol/L FA aqueous solution (red), 40 °C and 5 mol/L FA aqueous solution (blue). Reaction conditions: FA aqueous solution (13 mL), catalyst (2 mmol/L).

Table 1. Comparison of the FA dehydrogenation rate among the catalysts.[a]

Entry	Catalyst	Catalyst concentration /(mmol/L)	TOF at 40 MPa /(1/h)[b]	Reaction time /h	Pressure effect /-[c]
1	**1**	2.0	450	10	0.22
2	**2**	2.0	590	13	0.20
3	**2**	0.4	630	36	0.21
4	**3**	0.4	3130	7	0.24

[a] Reaction conditions: 60 °C, generated gas pressure: 40 MPa (H_2:CO_2 = 1:1), FA aqueous solution (16 mol/L, 40 ml). [b] Turnover frequency (TOF) is defined as the number of FA that converts into H_2 by one catalyst per hour, which was calculated from the gas generation rate. [c] Pressure effect represents the ratio of TOF at 40 MPa to that at atmospheric pressure.

In the case of catalyst **3**, the chelating conformation maintains in the complex when the imidazoline moiety rotates around pyridyl-imidazoline bond. Therefore, the catalytic activity of catalyst **3** can be retained at the pressure as high as 153 MPa. At 40 °C, 92 mol% of FA conversion with the gas pressure of 25 MPa was obtained from 5 mol/L FA aqueous solution. Although the presence of bases such as amine can accelerate the rate of FA dehydrogenation, only 44 mol% of FA was converted to H_2 and CO_2 in the presence of trimethylamine as a co-catalyst, and the attained pressure reduced to 4 MPa under the same condition.[45] This significant reduction of FA conversion and the attained pressure may be attributed to the formation of FA-base complexes with trimethylamine, which causes an increase in the Gibbs energy of reaction.[46] The generation of high-pressure H_2 by FA decomposition with high conversion can be achieved in the absence of bases.

The dehydrogenation rates of FA were compared among the catalysts **1**, **2** and **3** at 40MPa of the gas pressure (Table 1). For all the catalysts, the dehydrogenation rate remained constant in the beginning of the reaction, whereas it decreased with time as the FA concentration decreased (Figure S1 in the Supplementary Information). For the catalyst **2**, the FA dehydrogenation was slightly faster, but took longer time to reach equilibrium than **1** due to the precipitation of the catalyst (entries 1 and 2 in Table 1), which is caused by an increase in the pH of solution during the reaction.[37] Using the catalyst **3**, the reaction was completed quickly compared to the other catalysts, and the high TOF value of 3130 h^{-1} was obtained at 60 °C and 40 MPa (entry 4 in Table 1). Interestingly, regardless of the catalyst, the reaction rate under the high-pressure condition of 40 MPa decreased to about 1/5 from that of atmospheric pressure. This trend indicates that the effect of gas pressure to the reaction rate is similar among the studied catalysts. The activation energy (E_a) of **3** was determined from the Arrhenius plot under the high-pressure conditions (Figure S2 and Table S1 in the Supplementary Information). The calculated value of E_a at 40 MPa (74 kJ/mol) is almost same as that of at atmospheric condition (72 kJ/mol), which agrees with the results of **1**.[38] The pressure of generated gas by FA decomposition barely affects the catalytic reaction mechanism under the applied conditions.

Using the catalyst **3**, the continuous production of high-pressure H_2 by FA decomposition was performed at mild temperatures. After stopping the gas generation, neat FA was added to the reaction solution at a constant rate by a high-pressure liquid pump (Figure S3 in the Supplementary Information). The added FA was continuously and selectively

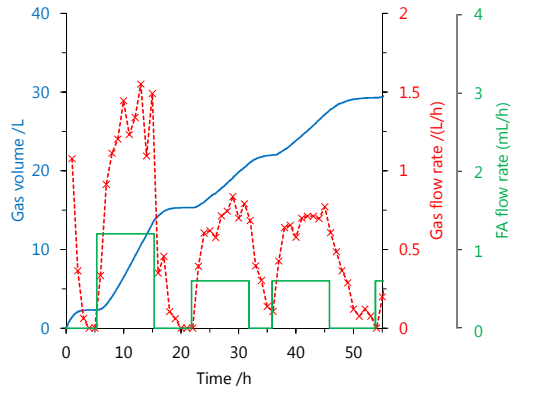

Figure 4. Generation rate and time of high-pressure gas controlled by neat FA addition: gas volume (blue; solid line), gas rate (red; cross), FA addition rate (green; soli line). Reaction condition: 50 °C, 20 MPa, initial FA aqueous solution (5 mol/L, 40 mL), FA addition rate (0.6-1.2 mL/h), catalyst **3** (16 μmol). Time starts after reaching the pressure.

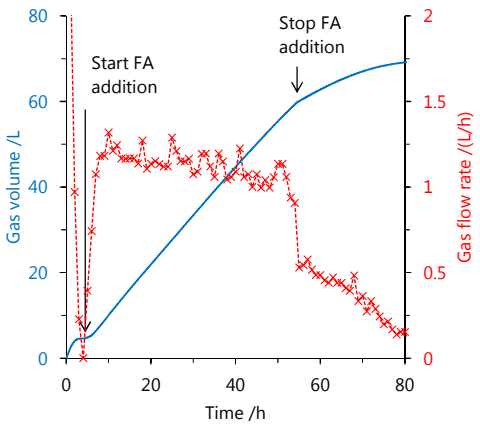

Figure 5. Continuous decomposition of FA at high pressure: gas volume (blue; solid line), gas rate (red; cross). Reaction condition: 60 °C, 40 MPa, initial FA aqueous solution (8 mol/L, 40 mL), FA addition (1.2 mL/h, 50 h), catalyst **3** (16 μmol). Time starts after reaching the pressure.

Table 2. Continuous decomposition of FA using the catalyst **3**.[a]

Entry	Pressure /MPa	FA flow rate /(mL/h)[b]	Stability /h[c]	Gas generation rate /(L/h)[d]	CO /vol. ppm	TON /-[e]
1	20	0.6	30	0.65±0.14	n.d.[h]	35 400
2[f]	20	0.6	<10	0.53±0.09	13±6	17 200
3[g]	20	0.6	30	0.68±0.14	46±23	36 900
4	20	1.2	20	1.36±0.14	n.d.	45 000
5	0.1	1.2	≥100	1.58±0.24	n.d.	198 500
6	40	0.6	20	0.54±0.11	n.d.	30 500

[a] Reaction conditions: 50 °C, initial FA aqueous solution (5 mol/L for 20 MPa and 8 mol/L for 40 MPa, 40 mL), catalyst (16 μmol). [b] FA was continuously added over 10 h and then stopped for several hours. [c] Time lapsed from the beginning until a decrease in the gas generation rate. [d] Average value during the continuous gas generation. [e] Turnover number (TON) is defined as the number of FA that converts into H_2 by one catalyst, which was calculated from the total volume of gas release. [f] Sodium formate was added to the initial FA solution (FA/SF = 10/1 mol/mol). [g] Temperature was 70 °C. [h] Below the detection limit (<2 vol. ppm).

decomposed into H_2 and CO_2 under the high-pressure conditions (Figures 4 and 5). The generation rate of high-pressure gas can be controlled by the FA feeding rate, and the stop-and-flow gas production experiments can be successfully demonstrated by the injection of FA keeping the high-pressure (Figure 4 and Table S3 in the Supplementary Information). Furthermore, when FA was added to the reaction system over 50 h at 40 MPa, the high-pressure H_2 was continuously generated with the low amount of CO (below 12 vol. ppm) at 60 °C (Figure 5). The generation rate of high-pressure gas was remain constant until initial 30 h, but the rate gradually decreased with duration of the FA addition and the gas generation continued even after the stop of FA feeding. The catalytic activity of **3** appears to be lost very slowly under the high-pressure conditions. The gas generation rate decreased very slowly with catalyst **3**, during the addition of high-pressure FA than compare to the catalyst **1** (Figure S4 in the Supplementary Information).

To further examine the stability of catalyst **3** at high pressures, the constant addition of high-pressure FA over 10 h was repeated for several times after stopping the gas generation by FA decomposition at 50 °C (Table 2 and Table S3 in the Supplementary Information). When the rate of FA addition was set to 0.6 mL/h at 20 MPa, the gas generation rate remained constant until 3 times of FA addition (entry 1 in Table 2). However, CO was observed in the gas generated at the forth times of FA addition. The catalyst **3** was stable over 30 h under the applied condition. In the presence of sodium formate (SF), the high-pressure gas was generated slower than in the absence of SF and CO was formed in the gas generated even at the first time of FA addition (entry 2 in Table 2). The reaction temperature barely affects the catalyst stability under the applied conditions, but higher temperature accelerated the formation of CO (entry 3 in Table 2). We therefore hypothesized that CO may be formed by the thermal decomposition of FA due to the catalyst deactivation. When the FA addition rate was changed from 0.6 to 1.2 mL/h, the gas generation rate increased about two times compared to the previous one, though the catalyst stability decreased with the increased rate of FA addition (entry 4 in Table 2). The TOF value from the gas generation rate was calculated as 1700 h^{-1}, which is about 7 times higher compared to the Ru complex catalyst tested under the milder temperature (230 h^{-1} at 100 °C).[31] The catalytic activity at 20 MPa started to decrease when the turnover number (TON) exceeded 40,000-50,000. Under atmospheric condition, FA was selectively dehydrogenated over 100 h at the constant rate, which corresponded to the TON value of 200 thousand (entry 5 in Table 2). When the gas pressure was 40 MPa, the generation rate of CO-free gas was kept constant over 20 h (entry 6 in Table 2). The gas pressure seems to affect the catalyst stability of **3**. When the catalyst was exposed to the gas product at high pressures, the catalytic activity was gradually lost with the time of high-pressure gas generation (Figure S5 in the Supplementary Information). After the completion of the reaction, the formation of insoluble compounds was not observed and *N*, *N*'-bidentate ligand was detected in the solution (Figure S6 and S7 in the Supplementary Information). The ligand elimination from the complex might cause a decrease in the catalytic activity at high pressures.[39] Further investigations on catalyst deactivation are under way.

The high-pressure H_2 can be produced by FA decomposition in the presence of catalyst, however, the separation of H_2 and CO_2 after the reaction is required for the hydrogen storage using CO_2 and the application to PEM fuel cells. When high-pressure H_2 is released, it should be cooled in advance to prevent from igniting due to the negative value of Joule-Thomson coefficient, as in hydrogen fuelling stations.[47] Therefore, the gas cooling unit is inevitable in the application of high-pressure H_2. The decrease in gas temperature during depressurization can reduce the energy required for cooling down the product gases from reaction temperature (Table S3 and Process Simulation in the Supplementary Information). According to the phase diagram of H_2 and CO_2 gas mixture, the vapor-liquid phase separation occurs at high pressures and low temperatures.[48, 49] The vapor phase mainly consists of H_2 whereas the liquid contains more CO_2 than H_2 under the conditions applied. Previously, we obtained 85 mol% of H_2 gas from FA using the vapor-liquid phase separation of FA decomposition gas (H_2:CO_2 = 1:1) at the low temperature.[36] The content of H_2 in the gas mixture increased with a decrease in the separator temperature. In this work, the FA decomposition gas was cooled to low temperatures that CO_2 forms a solid aiming for the production of highly concentrated

H_2 gas and the recovery of CO_2 under high-pressure conditions (Table 3). The high-pressure gas was generated by FA

Table 3. Separation of H_2 and CO_2 from the gas generated by FA decomposition at different temperatures of the separator.[a]

Entry	Pressure /MPa	Separator temperature /°C	Composition /mol%		Recovery /mol%[c]	
			H_2 in vapor phase	CO_2 in liquid phase[b]	H_2 as gas	CO_2 as liquid
1	40	rt	49±2	-	-	-
2[d]	30	-15	69	-	-	-
3	11	-78	96±1	>99	>99	94±6
4	27	-78	81±1	99±1	>99	69±5

[a] Reaction conditions: 60 °C, FA aqueous solution (8 mol/L, 40 mL), catalyst **3** (0.2 mmol/L). [b] Gas was obtained by heating the separator to room temperature after the high-pressure gas release during the separation was cooled. [c] Recovery is defined as the rate of H_2 as a gas and CO_2 as a liquid recovered from FA decomposition gas (H_2:CO_2 = 1:1). [d] Data was taken from previous work.[36]

decomposition using **3** at 60 °C, and then transferred to the separator cooled at -78 °C, while maintaining the pressure. The pressure drop was observed from 13 to 12 MPa when cooling the separator from -60 to -70 °C (Figure S8 in the Supplementary Information), which indicates the formation of solid state. The gas composition was analyzed during depressurization from 11 MPa to atmospheric pressure. More than 95 mol% H_2 gas was continuously obtained during the depressurization while keeping the separator cool (entry 3 in Table 3 and Figure S9 in the Supplementary Information). After depressurizing to atmospheric pressure, the separator was closed and heated to room temperature. The separator pressure increased up to 5.2 MPa at 16 °C. The high-pressure gas in separator was composed of >99 mol% CO_2 with less than 1 mol% H_2. The attained pressure in separator corresponds with the saturated pressure of CO_2 at 16 °C.[50] Thus, when the separator temperature was -78 °C, the FA decomposition gas was separated into H_2 gas and CO_2 solid with its concentration above 90 mol% in both phases. CO_2 can be recovered as a liquid by heating to room temperature without any mechanical compression. Furthermore, both H_2 and CO_2 were separately recovered from FA with >99 mol% and 94 % yield as a gas and liquid, respectively. When the gas pressure was increased from 11 to 27 MPa, the pressure drop occurred at the mild temperature (Figure S8b in the Supplementary Information), and the CO_2 recovery yield decreased to 69 mol% due to an increase of the CO_2 concentration in the vapor phase at 27 MPa.[48]

Conclusions

In conclusion, we investigated the sequential production of high-pressure H_2 by catalytic decomposition of FA and H_2/CO_2 separation towards the development of FA/CO_2 system as a hydrogen carrier and the application in PEM fuel cells. Using an Ir aqua complex **3**, the FA added to the reaction system was continuously and selectively decomposed into H_2 and CO_2 under the high-pressure conditions. The neat FA feeding is capable of controlling the generation time and rate of high-pressure H_2 for the on-demand production. Furthermore, well purified H_2 gas (96 mol%) and CO_2 liquid (>99 mol%) were obtained by cooling the gas generated from FA decomposition after the reaction while maintaining the pressure. The recovery of CO_2 in the liquid state without any mechanical compression gives advantages on the delivery and storage, which could be the source of hydrogen carrier. This work suggests that the FA decomposition at high pressures can lead the effective separation of H_2 and CO_2 after the reaction as well as can increase volumetric energy density of H_2.

Methods

General. The Ir aqua complexes, [Cp*Ir(4,4'-dihydroxy-2,2'-bipyridine)(H_2O)][SO_4] (**1**),[51] [Cp*Ir(4,7-dihydroxy-1,10-phenanthroline)(H_2O)][SO_4] (**2**)[52] and [Cp*Ir(2-(2'-pyridinyl)-4,5-dihydro-1*H*-imidazole)(H_2O)][SO_4] (**3**),[53] were prepared according to the literature. Formic acid (FA, >99.0 %) and sodium formate (SF, >99.0 %) were used as received from Wako Pure Chemical Industries, Ltd. Deionized water was purified through filtration system (EMD Millipore Corp., ZFSQ240P4) and water distillation system (Toyo Roshi Kaisha, Ltd., GS-590). All reagents were degassed by bubbling helium gas before use.

The decomposition of FA and separation of the generated gas under high-pressure conditions were carried out using the same apparatus described in our previous work except the valve between the reactor and the separator.[36] For the appropriate evaluation of H_2/CO_2 gas separation, it is necessary to prevent the line blocking by solid CO_2 or overflowing at the separator due to the transfer of high-pressure gas. As a solution, we set a valve, which can control the high-pressure gas transfer rate from the batch reactor to the separator. The aqueous solution of the catalyst and FA were loaded into a reactor (50 ml) at room temperature, then the reaction solution was started to stirring and heated to the desired temperature. The pressure of generated gas was monitored by the pressure sensor (PGM-500KH, Kyowa Electronic Instruments Co., Ltd.). The gas pressure was controlled by a back-pressure regulator (JASCO Corp., BP-2080). The volume of gas release was measured by a wet gas meter (Shinagawa Co., Ltd., W-NK-0.5A), and the gas composition was monitored using a GC-μTCD system (Agilent Technologies, 3000A Micro GC). A TOF value was determined from an average rate of gas generation using the ideal gas law. In the GC analysis, the

detection limits and quantification were calculated from the uncertainty measurement with the coverage factor k = 3 and 10, respectively. For testing the continuous gas generation, neat FA was constantly introduced to the reaction solution by a liquid pump (JASCO Corp., PU-980) under high-pressure conditions (Figure S3 in the Supplementary Information). After completion of the reaction, the reactor was cooled and then depressurized carefully to atmospheric pressure. A HPLC-UV system on an ion exclusion column (Showa Denko K. K., KC-811; 0.02 mol/L phosphoric acid aqueous solution) was used to determine the FA concentration in reaction solution. The conversion of FA was reported as the mean value of the residual FA concentration in the reaction solution and the volume of gas generated by FA decomposition. The analysis of reaction solution was measured with an electrospray ionization mass spectrometry (ESI-MS) in a positive ion mode (Agilent Technologies, 6224 TOF LC/MS; methanol/water = 1/1 v/v).

Conflicts of interest

The authors declare no conflicts of interest.

Acknowledgements

The authors acknowledge the financial support of Japan Science and Technology Agency (JST), CREST (No. JPMJCR1342), and the International Joint Research Program for Innovative Energy Technology of the Ministry of Economy, Trade, and Industry (METI) of Japan.

References

1. U. Eberle, M. Felderhoff and F. Schüth, *Angew. Chem., Int. Ed.*, 2009, **48**, 6608-6630.
2. N. Armaroli and V. Balzani, *ChemSusChem*, 2011, **4**, 21-36.
3. A. F. Dalebrook, W. Gan, M. Grasemann, S. Moret and G. Laurenczy, *Chem. Commun.*, 2013, **49**, 8735-8751.
4. S. Niaz, T. Manzoor and A. H. Pandith, *Renewable Sustainable Energy Rev.*, 2015, **50**, 457-469.
5. M. Grasemann and G. Laurenczy, *Energy Environ. Sci.*, 2012, **5**, 8171-8181.
6. A. K. Singh, S. Singh and A. Kumar, *Catal. Sci. Technol.*, 2016, **6**, 12-40.
7. D. Mellmann, P. Sponholz, H. Junge and M. Beller, *Chem. Soc. Rev.*, 2016, **45**, 3954-3988.
8. J. Eppinger and K.-W. Huang, *ACS Energy Lett.*, 2017, **2**, 188-195.
9. K. Sordakis, C. Tang, L. K. Vogt, H. Junge, P. J. Dyson, M. Beller and G. Laurenczy, *Chem. Rev.*, 2018, **118**, 372-433.
10. H. Kawanami, Y. Himeda and G. Laurenczy, in *Advances in Inorganic Chemistry*, eds. E. Rudi van and D. H. Colin, Academic Press, 2017, vol. 70, pp. 395-427.
11. H. Zhong, M. Iguchi, M. Chatterjee, Y. Himeda, Q. Xu and H. Kawanami, *Advanced Sustainable Systems*, 2018, **2**, 1700161.
12. W.-H. Wang, Y. Himeda, J. T. Muckerman, G. F. Manbeck and E. Fujita, *Chem. Rev.*, 2015, **115**, 12936-12973.
13. J. Klankermayer, S. Wesselbaum, K. Beydoun and W. Leitner, *Angew. Chem., Int. Ed.*, 2016, **55**, 7296-7343.
14. D. Bulushev and J. R. H. Ross, *ChemSusChem*, 2018, **11**, 821-836.
15. P. G. Jessop, in *The Handbook of Homogeneous Hydrogenation*, eds. J. G. d. Vries and C. J. Elsevier, Wiley-VCH Verlag GmbH, Weinheim, 2008, DOI: 10.1002/9783527619382.ch17, ch. 17, pp. 489-511.
16. A. Boddien, B. Loges, H. Junge and M. Beller, *ChemSusChem*, 2008, **1**, 751-758.
17. A. Majewski, D. J. Morris, K. Kendall and M. Wills, *ChemSusChem*, 2010, **3**, 431-434.
18. M. Czaun, J. Kothandaraman, A. Goeppert, B. Yang, S. Greenberg, R. B. May, G. A. Olah and G. K. S. Prakash, *ACS Catal.*, 2016, **6**, 7475-7484.
19. I. Mellone, F. Bertini, M. Peruzzini and L. Gonsalvi, *Catal. Sci. Technol.*, 2016, **6**, 6504-6512.
20. L. Piola, J. A. Fernández-Salas, F. Nahra, A. Poater, L. Cavallo and S. P. Nolan, *Mol. Catal.*, 2017, **440**, 184-189.
21. I. Yuranov, N. Autissier, K. Sordakis, A. F. Dalebrook, M. Grasemann, V. Orava, P. Cendula, L. Gubler and G. Laurenczy, *ACS Sustainable Chem. Eng.*, 2018, **6**, 6635-6643.
22. T. Tingelöf, L. Hedström, N. Holmström, P. Alvfors and G. Lindbergh, *Int. J. Hydrogen Energy*, 2008, **33**, 2064-2072.
23. N. Zamel and X. Li, *Prog. Energy Combust. Sci.*, 2011, **37**, 292-329.
24. M. A. Díaz, A. Iranzo, F. Rosa, F. Isorna, E. López and J. P. Bolivar, *Energy*, 2015, **90**, 299-309.
25. M. Voldsund, K. Jordal and R. Anantharaman, *Int. J. Hydrogen Energy*, 2016, **41**, 4969-4992.
26. M. Felderhoff, C. Weidenthaler, R. von Helmolt and U. Eberle, *Phys. Chem. Chem. Phys.*, 2007, **9**, 2643-2653.
27. C. Fellay, P. J. Dyson and G. Laurenczy, *Angew. Chem., Int. Ed.*, 2008, **47**, 3966-3968.
28. B. Loges, A. Boddien, H. Junge and M. Beller, *Angew. Chem., Int. Ed.*, 2008, **47**, 3962-3965.
29. Z. Wang, S.-M. Lu, J. Li, J. Wang and C. Li, *Chem. - Eur. J.*, 2015, **21**, 12592-12595.
30. J. J. A. Celaje, Z. Lu, E. A. Kedzie, N. J. Terrile, J. N. Lo and T. J. Williams, *Nat. Commun.*, 2016, **7**.
31. C. Fellay, N. Yan, P. J. Dyson and G. Laurenczy, *Chem. - Eur. J.*, 2009, **15**, 3752-3760.
32. M. Czaun, A. Goeppert, J. Kothandaraman, R. B. May, R. Haiges, G. K. S. Prakash and G. A. Olah, *ACS Catal.*, 2014, **4**, 311-320.
33. G. Papp, G. Olveti, H. Horvath, A. Katho and F. Joo, *Dalton Trans.*, 2016, **45**, 14516-14519.
34. C. Guan, D.-D. Zhang, Y. Pan, M. Iguchi, M. J. Ajitha, J. Hu, H. Li, C. Yao, M.-H. Huang, S. Min, J. Zheng, Y. Himeda, H. Kawanami and K.-W. Huang, *Inorg. Chem.*, 2017, **56**, 438-445.
35. H. Zhong, M. Iguchi, F.-Z. Song, M. Chatterjee, T. Ishizaka, I. Nagao, Q. Xu and H. Kawanami, *Sustainable Energy Fuels*, 2017, **1**, 1049-1055.
36. M. Iguchi, Y. Himeda, Y. Manaka, K. Matsuoka and H. Kawanami, *ChemCatChem*, 2016, **8**, 886-890.
37. M. Iguchi, Y. Himeda, Y. Manaka and H. Kawanami, *ChemSusChem*, 2016, **9**, 2749-2753.
38. M. Iguchi, H. Zhong, Y. Himeda and H. Kawanami, *Chem. - Eur. J.*, 2017, **23**, 17017-17021.

39. M. Iguchi, H. Zhong, Y. Himeda and H. Kawanami, *Chem. - Eur. J.*, 2017, **23**, 17788-17793.
40. P. Sponholz, D. Mellmann, H. Junge and M. Beller, *ChemSusChem*, 2013, **6**, 1172-1176.
41. A. Boddien, B. Loges, H. Junge, F. Gärtner, J. R. Noyes and M. Beller, *Adv. Synth. Catal.*, 2009, **351**, 2517-2520.
42. T. H. Oh, *Energy*, 2016, **112**, 679-685.
43. V. Henricks, I. Yuranov, N. Autissier and G. Laurenczy, *Catalysts*, 2017, **7**, 348.
44. N. Onishi, M. Z. Ertem, S. Xu, A. Tsurusaki, Y. Manaka, J. T. Muckerman, E. Fujita and Y. Himeda, *Catal. Sci. Technol.*, 2016, **6**, 988-992.
45. K. Sordakis, M. Beller and G. Laurenczy, *ChemCatChem*, 2014, **6**, 96-99.
46. C. Fink, S. Katsyuba and G. Laurenczy, *Phys. Chem. Chem. Phys.*, 2016, **18**, 10764-10773.
47. J. Alazemi and J. Andrews, *Renewable Sustainable Energy Rev.*, 2015, **48**, 483-499.
48. C. Y. Tsang and W. B. Street, *Chem. Eng. Sci.*, 1981, **36**, 993-1000.
49. O. Fandiño, J. P. M. Trusler and D. Vega-Maza, *Int. J. Greenhouse Gas Control*, 2015, **36**, 78-92.
50. R. Span and W. Wagner, *J. Phys. Chem. Ref. Data*, 1996, **25**, 1509-1596.
51. Y. Himeda, N. Onozawa-Komatsuzaki, S. Miyazawa, H. Sugihara, T. Hirose and K. Kasuga, *Chem. - Eur. J.*, 2008, **14**, 11076-11081.
52. Y. Himeda, N. Onozawa-Komatsuzaki, H. Sugihara and K. Kasuga, *Organometallics*, 2007, **26**, 702-712.
53. S. Xu, N. Onishi, A. Tsurusaki, Y. Manaka, W.-H. Wang, J. T. Muckerman, E. Fujita and Y. Himeda, *Eur. J. Inorg. Chem.*, 2015, **2015**, 5591-5594.

Table of Contents Entry

Table of Contents Entry